Design and optimization of CMOS LNA with ESD protection for 2.4 GHz WSN application*

Li Zhiqun(李智群)[1, 2, 3, †], Chen Liang(陈亮)[1, 2, 3], and Zhang Hao(张浩)[1, 2]

[1]Institute of RF- & OE- ICs, Southeast University, Nanjing 210096, China
[2]RFIC and System Engineering Research Center of Ministry of Education of China, Southeast University, Nanjing 210096, China
[3]Research Center of Sensor Network Technology, Southeast University, Wuxi 214135, China

Abstract: A new optimization method of a source inductive degenerated low noise amplifier (LNA) with electrostatic discharge protection is proposed. It can achieve power-constrained simultaneous noise and input matching. An analysis of the input impedance and the noise parameters is also given. Based on the developed method, a 2.4 GHz LNA for wireless sensor network application is designed and optimized using 0.18-μm RF CMOS technology. The measured results show that the LNA achieves a noise figure of 1.59 dB, a power gain of 14.12 dB, an input 1 dB compression point of –8 dBm and an input third-order intercept point of 1 dBm. The DC current is 4 mA under a supply of 1.8 V.

Key words: LNA; ESD protection; noise and input impedance matching; CMOS

DOI: 10.1088/1674-4926/32/10/105004 **EEACC:** 2570

1. Introduction

The low noise amplifier (LNA) is one of the key components in most communication systems, because it is the first active block after the antenna and determines the dynamic range of the receiver. The conventional inductively degenerated common source LNA is very popular for narrow band applications. For this topology, there are several optimization methods proposed in published studies[1, 2], such as the power-constrained simultaneous noise and input matching (PCSNIM) technique proposed in Ref. [2]. However, this ignored the effect of the input parasitic capacitance of the electrostatic discharge (ESD) protection circuits and the pad (usually very small compared to the ESDs). Considering the reliability of products, the ESD protection of a chip is very important and necessary. At radio frequency, the parasitic capacitance of the input port has a significant effect on the performance of the LNA[3], such as noise figure, power gain, and so on. Thus, it must be taken into account in the circuit design. Sivonen[4] has proposed an ESD and LNA co-design method. Its biggest drawback is that it needs two off-chip lumped components to realize the input power matching, which will increase the design complexity and the system cost.

In this paper, a source inductive degenerated LNA with ESD is analyzed in detail. An optimization method, which can achieve ESD protected LNA power-constrained simultaneous noise and input matching, is described. It features also the fact that only one off-chip lumped component is needed. An LNA is designed and measured using 0.18-μm RF CMOS technology. The measured results show that the LNA achieves an NF of 1.59 dB and a power gain of 14.12 dB.

2. Circuit analysis

2.1. Input power matching of LNA with ESD

The circuit of the LNA with ESD consisting of two reverse biased diodes is shown in Fig. 1(a), and Figure 1(b) shows its small signal equivalent circuit, in which $C_{\rm p}$ represents the parasitic capacitance of the ESD and the input pad, while $L_{\rm g}$ consists of the bonding wire inductor connecting chip pad and PCB and the SMT inductor on PCB.

As shown in Fig. 1(b), the input impedance looking into the gate of M1 can be expressed as

$$Z'_{\rm in} = \frac{1}{Y'_{\rm in}} = sL_{\rm s} + \frac{1}{sC_{\rm t}} + \frac{g_{\rm m}L_{\rm s}}{C_{\rm t}} = \frac{1}{sC_1} + R_{\rm eq}, \quad (1)$$

where

$$C_{\rm t} = C_{\rm gs} + C_{\rm ex}, \frac{1}{C_1} = \frac{1}{C_{\rm t}} - \omega^2 L_{\rm s}, R_{\rm eq} = \frac{g_{\rm m}L_{\rm s}}{C_{\rm t}}, s = j^*\omega.$$

Through a series of parallel-series and series-parallel conversions, as shown in Fig. 2, we have

$$\begin{aligned}\mathrm{Re}[Z_{\rm in}] = R_3 &\approx \frac{1}{R_2\,(\omega C_2)^2} \approx \frac{1}{\dfrac{1}{R_{\rm eq}\,(\omega C_1)^2}\omega^2(C_1+C_{\rm p})^2}\\ &= R_{\rm eq}\left(\frac{C_1}{C_1+C_{\rm p}}\right)^2 = \frac{g_{\rm m}L_{\rm s}}{C_{\rm t}}\left(\frac{C_1}{C_1+C_{\rm p}}\right)^2,\end{aligned} \quad (2)$$

* Project supported by the National High Technology Research and Development Program of China (No. 2007AA01Z2A7) and the 5th Program of Six Talent Summits of Jiangsu Province, China.
† Corresponding author. Email: zhiqunli@seu.edu.cn
Received 17 April 2011, revised manuscript received 25 May 2011

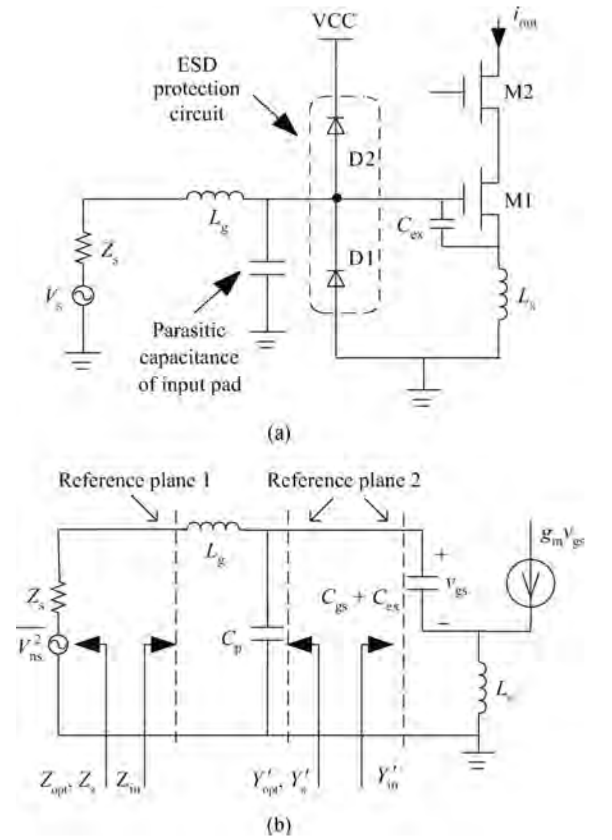

Fig. 1. (a) Circuit of LNA with ESD. (b) Its small-signal equivalent circuit.

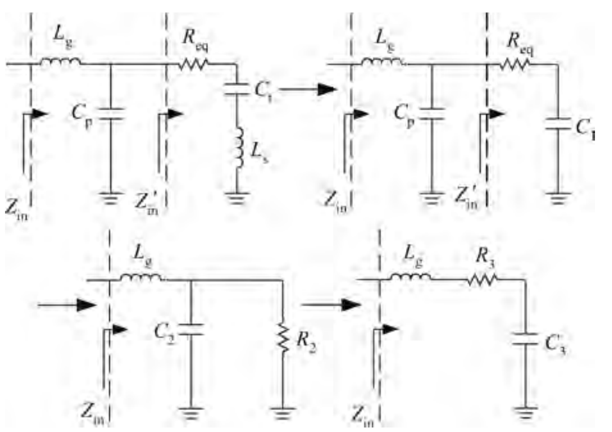

Fig. 2. Input impedance conversion.

$$\mathrm{Im}[Z_{\mathrm{in}}] = sL_{\mathrm{g}} + \frac{1}{sC_3} \approx \frac{\dfrac{1}{sC_{\mathrm{t}}} + sL_{\mathrm{s}}}{1 + sC_{\mathrm{p}}\left(\dfrac{1}{sC_{\mathrm{t}}} + L_{\mathrm{s}}\right)} + sL_{\mathrm{g}}. \quad (3)$$

And the power matching requirement is that

$$\begin{cases} \mathrm{Re}[Z_{\mathrm{in}}] = \mathrm{Re}[Z_{\mathrm{s}}], \\ \mathrm{Im}[Z_{\mathrm{in}}] = -\mathrm{Im}[Z_{\mathrm{s}}]. \end{cases} \quad (4)$$

From Eq. (2), it can be seen that the parallel parasitic capacitance C_{p} transforms downwards the real part of the input impedance, and the simulation results are shown in Fig. 3 with $C_{\mathrm{ex}} = 0$. The real part of Z_{in} is below 30 Ω for $C_{\mathrm{p}} > 230$ fF, which is unacceptable for a 50 Ω system. Very small mismatch of $\mathrm{Im}[Z_{\mathrm{in}}]$ will make S_{11} be above –10 dB. C_{ex} is very important in solving this problem as will be shown in next paragraph.

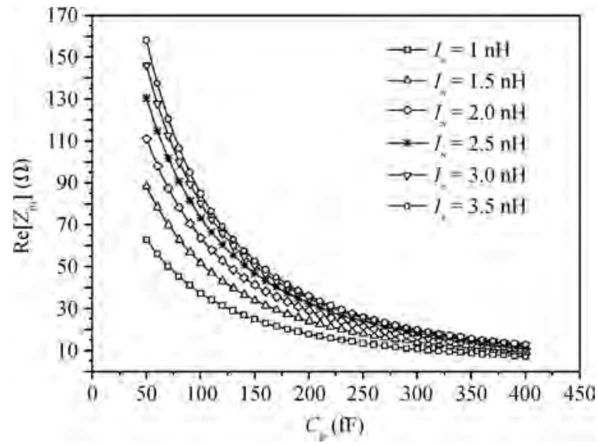

Fig. 3. Effect of C_{p} on the real part of the input impedance.

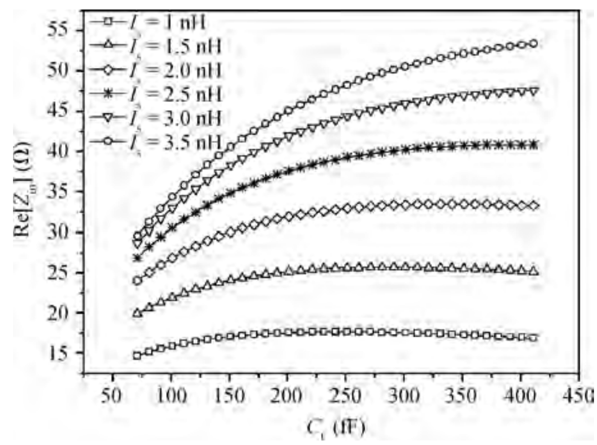

Fig. 4. Effect of C_{t} on the $\mathrm{Re}[Z_{\mathrm{in}}]$.

We substitute C_1 in Eq. (2) with its expression, and then we get the following equation,

$$\mathrm{Re}[Z_{\mathrm{in}}] = \frac{g_{\mathrm{m}}L_{\mathrm{s}}}{\dfrac{a^2}{C_{\mathrm{t}}} + b^2C_{\mathrm{t}} + 2ab}, \quad (5)$$

where $a = C_{\mathrm{p}}$, $b = 1 - \omega^2 L_{\mathrm{s}} C_{\mathrm{p}}$.

From Eq. (5), it can be seen that $\mathrm{Re}[Z_{\mathrm{in}}]$ increases as the C_{t} increases when $C_{\mathrm{t}} < a/b$, as shown in Fig. 4. This is quite different from that of the CS LNA without ESD, in which the effect of C_{t} is only reducing the real part of the input impedance and is taken advantage of in the input power match. There are two ways to increase C_{t}. One is by increasing C_{gs} and the other is by increasing C_{ex}. Exploiting the first method will increase the power consumption. So, C_{ex} is increased to match the real part of the input impedance to 50 Ω, and the real part of the input impedance matching could be achieved by choosing appropriate g_{m}, L_{s} and C_{ex}.

According to Eq. (4), the inductor L_{g} must be selected as

$$L_{\mathrm{g}}=\frac{1}{C_{3}\omega^{2}}=\left[\omega^{2}\left(\frac{C_{\mathrm{t}}}{1-\omega^{2}C_{\mathrm{t}}L_{\mathrm{s}}}+C_{\mathrm{p}}\right)\right]^{-1}. \quad (6)$$

In this method, a single off-chip component L_{g} can make the input port matching to 50 Ω.

2.2. ESD protected LNA's power-constrained simultaneous noise and input power matching

After a complex derivation (the detailed derivation is shown in Appendix A), the optimum source admittance (Y'_{opt}) of the circuit shown in Fig. 1(b) can be given by

$$Y'_{\mathrm{opt}}=G_{\mathrm{opt}}+\mathrm{j}B_{\mathrm{opt}}, \quad (7)$$

where

$$\begin{aligned}B_{\mathrm{opt}}&=-B_{\mathrm{c}}\\&=-\left[\omega C_{\mathrm{t}}\left(\alpha|c|\sqrt{\frac{\delta}{5\gamma}}+1\right)-\omega^{3}C_{\mathrm{t}}^{2}L_{\mathrm{s}}\left(2\alpha|c|\sqrt{\frac{\delta}{5\gamma}}\right.\right.\\&\quad\left.\left.+1+\frac{\alpha^{2}\delta}{5\gamma}\right)\right]\left[1+\omega^{4}C_{\mathrm{t}}^{2}L_{\mathrm{s}}^{2}\left(2\alpha|c|\sqrt{\frac{\delta}{5\gamma}}+1+\frac{\alpha^{2}\delta}{5\gamma}\right)\right.\\&\quad\left.-2\omega^{2}C_{\mathrm{t}}L_{\mathrm{s}}\left(\alpha|c|\sqrt{\frac{\delta}{5\gamma}}+1\right)\right]^{-1},\end{aligned}$$

and

$$\begin{aligned}G_{\mathrm{opt}}=&\left[B_{\mathrm{c}}^{2}\omega^{4}C_{\mathrm{t}}^{2}L_{\mathrm{s}}^{2}\left(2\alpha|c|\sqrt{\frac{\delta}{5\gamma}}+\frac{\alpha^{2}\delta}{5\gamma}+1\right)\right.\\&+2B_{\mathrm{c}}\omega^{3}C_{\mathrm{t}}^{2}L_{\mathrm{s}}\left(2\alpha|c|\sqrt{\frac{\delta}{5\gamma}}+1+\frac{\alpha^{2}\delta}{5\gamma}\right)\\&-2B_{\mathrm{c}}^{2}\omega^{2}C_{\mathrm{t}}L_{\mathrm{s}}\left(\alpha|c|\sqrt{\frac{\delta}{5\gamma}}+1\right)+\omega^{2}C_{\mathrm{t}}^{2}\left(2\alpha|c|\sqrt{\frac{\delta}{5\gamma}}\right.\\&\left.\left.+1+\frac{\alpha^{2}\delta}{5\gamma}\right)-2B_{\mathrm{c}}\omega C_{\mathrm{t}}\left(\alpha|c|\sqrt{\frac{\delta}{5\gamma}}+1\right)+B_{\mathrm{c}}^{2}\right]^{1/2}\\&\times\left[1+\omega^{4}C_{\mathrm{t}}^{2}L_{\mathrm{s}}^{2}\left(2\alpha|c|\sqrt{\frac{\delta}{5\gamma}}+\frac{\alpha^{2}\delta}{5\gamma}+1\right)\right.\\&\left.-2\omega^{2}C_{\mathrm{t}}L_{\mathrm{s}}\left(\alpha|c|\sqrt{\frac{\delta}{5\gamma}}+1\right)\right]^{-1/2}.\end{aligned}$$

In order to achieve the ESD protected LNA's power-constrained simultaneous noise and input matching, the following equation must be satisfied,

$$Y'_{\mathrm{opt}}=Y'_{\mathrm{s}}, \quad (8)$$

where

$$Y'_{\mathrm{s}}=\frac{1}{Q^{2}R_{\mathrm{s}}}+\mathrm{j}\left(\omega C_{\mathrm{p}}-\frac{1}{\omega L_{\mathrm{g}}}\right),$$

and

$$Q=\frac{\omega L_{\mathrm{g}}}{R_{\mathrm{s}}}.$$

The two conditions that satisfy Eq. (8) are as follows, (1) $\mathrm{Re}[Y'_{\mathrm{opt}}]=\mathrm{Re}[Y'_{\mathrm{s}}]$:

$$\begin{aligned}&\left[B_{\mathrm{c}}^{2}\omega^{4}C_{\mathrm{t}}^{2}L_{\mathrm{s}}^{2}\left(2\alpha|c|\sqrt{\frac{\delta}{5\gamma}}+\frac{\alpha^{2}\delta}{5\gamma}+1\right)\right.\\&+2B_{\mathrm{c}}\omega^{3}C_{\mathrm{t}}^{2}L_{\mathrm{s}}\left(2\alpha|c|\sqrt{\frac{\delta}{5\gamma}}+1+\frac{\alpha^{2}\delta}{5\gamma}\right)\\&-2B_{\mathrm{c}}^{2}\omega^{2}C_{\mathrm{t}}L_{\mathrm{s}}\left(\alpha|c|\sqrt{\frac{\delta}{5\gamma}}+1\right)\\&+\omega^{2}C_{\mathrm{t}}^{2}\left(2\alpha|c|\sqrt{\frac{\delta}{5\gamma}}+1+\frac{\alpha^{2}\delta}{5\gamma}\right)\\&\left.-2B_{\mathrm{c}}\omega C_{\mathrm{t}}\left(\alpha|c|\sqrt{\frac{\delta}{5\gamma}}+1\right)+B_{\mathrm{c}}^{2}\right]^{1/2}\\&\times\left[1+\omega^{4}C_{\mathrm{t}}^{2}L_{\mathrm{s}}^{2}\left(2\alpha|c|\sqrt{\frac{\delta}{5\gamma}}+\frac{\alpha^{2}\delta}{5\gamma}+1\right)\right.\\&\left.-2\omega^{2}C_{\mathrm{t}}L_{\mathrm{s}}\left(\alpha|c|\sqrt{\frac{\delta}{5\gamma}}+1\right)\right]^{-1/2}\\&=\frac{1}{Q^{2}R_{\mathrm{s}}}.\end{aligned} \quad (9)$$

(2) $\mathrm{Im}[Y'_{\mathrm{opt}}]=\mathrm{Im}[Y'_{\mathrm{s}}]$:

$$\begin{aligned}&-\left\{\omega C_{\mathrm{t}}\left(\alpha|c|\sqrt{\frac{\delta}{5\gamma}}+1\right)-\omega^{3}C_{\mathrm{t}}^{2}L_{\mathrm{s}}\left(2\alpha|c|\sqrt{\frac{\delta}{5\gamma}}\right.\right.\\&\left.\left.+1+\frac{\alpha^{2}\delta}{5\gamma}\right)\right\}\left\{1+\omega^{4}C_{\mathrm{t}}^{2}L_{\mathrm{s}}^{2}\left(2\alpha|c|\sqrt{\frac{\delta}{5\gamma}}+1+\frac{\alpha^{2}\delta}{5\gamma}\right)\right.\\&\left.-2\omega^{2}C_{\mathrm{t}}L_{\mathrm{s}}\left(\alpha|c|\sqrt{\frac{\delta}{5\gamma}}+1\right)\right\}^{-1}\\&=\omega C_{\mathrm{p}}-\frac{1}{\omega L_{\mathrm{g}}}.\end{aligned} \quad (10)$$

To achieve ESD protected LNA's power-constrained simultaneous noise and input matching, Equations (4) and (8) must be satisfied simultaneously. Since there are four equations and five unknowns (g_{m}, C_{gs} or W, C_{ex}, L_{s}, L_{g}), Equations (4) and (8) can be solved for an arbitrary value of Z_{s} by fixing the power consumption of the LNA.

3. Circuit design and measured results

The design is based on a 0.18 μm RF CMOS technology. In order to acquire 2 kV HBM ESD protection, the value of the ESD parasitic capacitance is about 200 fF[5]. The input pad is only made of the top metal (M6) to reduce its parasitic capacitance. In this design, it is about 35 fF, so, the value of C_{p} is about 235 fF. The value of Z_{s} is 50 Ω. The supply voltage is

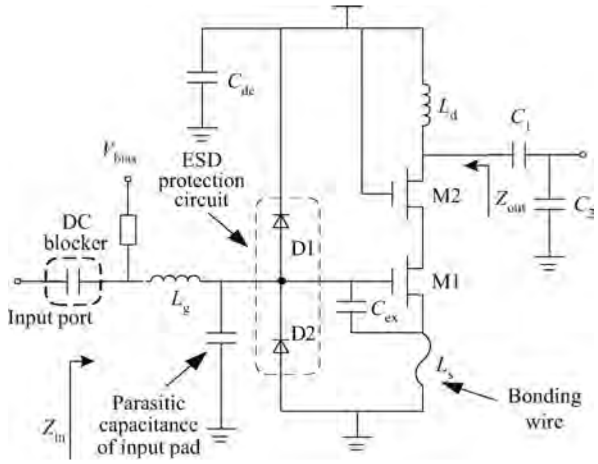

Fig. 5. Schematic of LNA with ESD protection circuit.

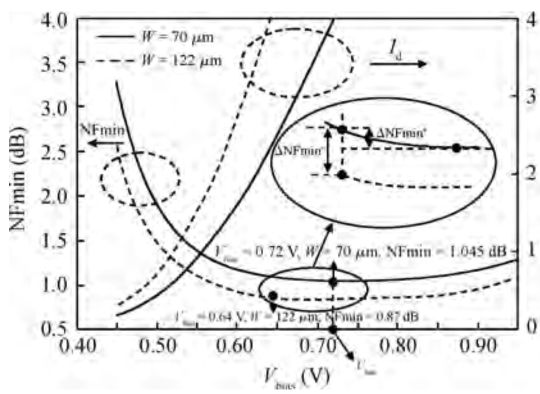

Fig. 6. DC current and NFmin versus V_{bias}.

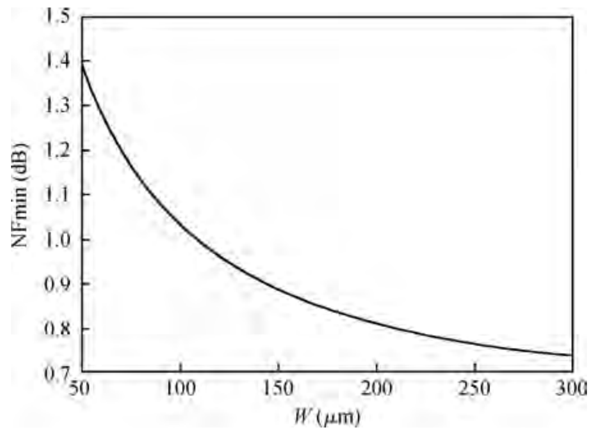

Fig. 7. NFmin versus W ($V_{\text{bias}} = 0.6$ V).

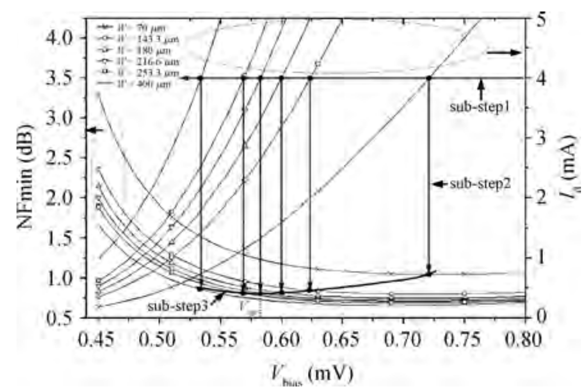

Fig. 8. DC current and NFmin versus V_{bias} relationship with different W.

fixed at 1.8 V and the power is constrained at 7.2 mW, so the DC current is constrained at 4 mA. The complete schematic of the LNA with an ESD protection circuit is shown in Fig. 5. Before the design of the LNA with ESD is described, the disadvantage of the PCSNIM[2] is analyzed.

3.1. Analysis of the disadvantage of PCSNIM technology

The choice of bias voltage (V_{bias}) and gate width (W) of the PCSNIM is divided into two steps. First, choose the DC-bias, for example, the bias point that provides minimum NFmin. Second, choose the transistor size based on the power constraint. With this method, an NFmin is obtained, but it is not the minimum one. Figure 6 shows the simulations of DC current and NFmin at 2.4 GHz versus Vbias. As Figure 6 shows, according to PCSNIM, NFmin gets its minimum value, when the V_{bias} is 0.72 V. Based on the 4 mA DC current (I_{d}) limit, then the W is determined to be 70 μm, and the NFmin is 1.045 dB at 2.4 GHz. But when the V_{bias} is 0.6437 V, W is 122 μm, current consumption is 4 mA and the NFmin is 0.87 dB, which is smaller than 1.045 dB. This problem exists in the design process of LNA both with ESD and without. The reason for this problem is described as follows. Because of the current limit, V_{bias} and W restrict each other. If V_{bias} decreases, W will increase. Figure 7 demonstrates that with an increase in W, NFmin decreases, and more and more slowly (at a constant V_{bias}). Furthermore, NFmin rises very slightly in the vicinity of the point $V_{\min}$ that provides the minimum NFmin (0.72 V in Fig. 6), and increases more and more quickly when V_{bias} decreases from point $V_{\min}$. So, let the variation in NFmin be analyzed when V_{bias} is reduced from $V_{\min}$ and W is increased (maintain a constant current consumption). Divide V_{bias} into a large number of steps; for example, 100, from $V_{\min}$ to V_{TH}. These steps are called $V_1, V_2, \ldots, V_n, \ldots, V_{100}$, with their corresponding W are $W_1, W_2, \ldots, W_n, \ldots, W_{100}$. When n is small, the increase in NFmin (ΔNFmin^+) due to the decrease in V_{bias} from V_n to V_{n+1} with the W of W_{n} is smaller than the decrease in NFmin (ΔNFmin^-) due to the increase in W from W_n to W_{n+1} at the bias voltage of V_{n+1} (shown in Fig. 6), then at one combination of W and V_{bias}, ΔNFmin^+ will equal ΔNFmin^-, and after that, ΔNFmin^+ will be greater than ΔNFmin^-. So NFmin falls at first, reaches its minimum value and then rises. As a result, this combination of W and V_{bias} will provide the real minimum NFmin with the power constraint. This method will be described in part B.

3.2. Circuit optimization technology of LNA with ESD

The designing of an LNA is processing at reference plane 1 in Fig. 1. The solutions of Eqs. (4) and (8) also satisfy the following equations,

$$\begin{cases} \text{Re}[Z_{\text{opt}}] = \text{Re}[Z_{\text{in}}] = 50, \\ \text{Im}[Z_{\text{opt}}] = \text{Im}[Z_{\text{in}}] = 0. \end{cases} \tag{11}$$

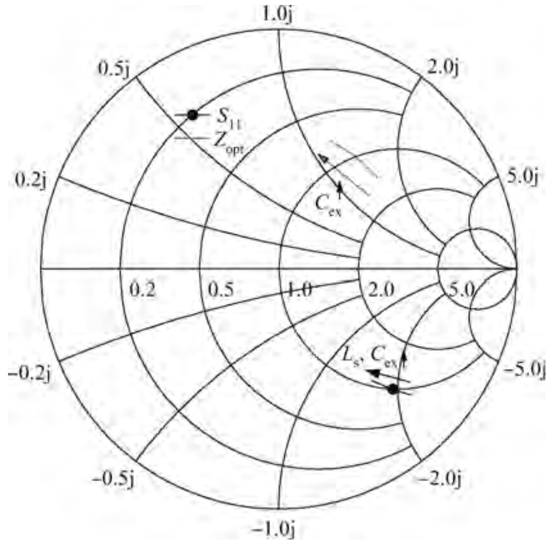

Fig. 9. Tune C_{ex} and L_s to satisfy $\mathrm{Re}[Z'_{opt}] = \mathrm{Re}[Z'_{in}] = R_s$.

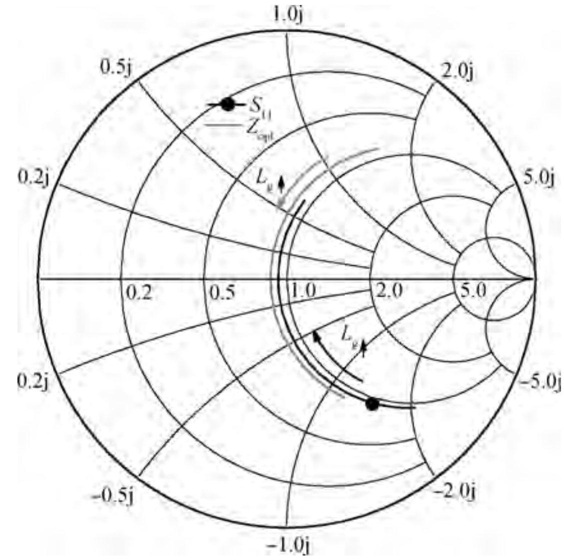

Fig. 10. Change process after setting L_g.

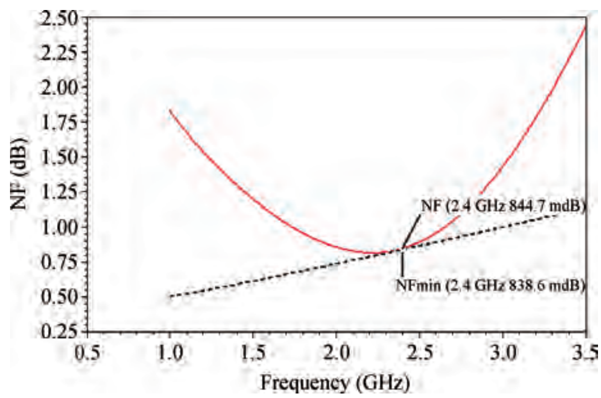

Fig. 11. Simulated NF and NFmin.

The design process of LNA with ESD is described as follows:

Step 1: Tune the size of the ESD circuit, and let the parasitic capacitance be equal to 200 fF. Add the ESD circuit into the LNA.

Step 2: Determine the DC-bias V_{bias} and the width W of M1 to provide the minimum NFmin. This step is divided into three sub-steps.

(1) Simulate the DC current and NFmin versus V_{bias} relationship with different W, respectively, and plot them in the same figure, as shown in Fig. 8. Then plot the constant I_d line of the maximum I_d (4 mA in this paper). This crosses with the DC current responses with different W. Mark these intersections. They represent the combinations of V_{bias} and W that meet the power requirement (4 mA). In Fig. 8, sub-step1 shows this step.

(2) Mark the intersections' corresponding points in the NFmin curves. In Fig. 8, sub-step 2 shows this step.

(3) String together these points to obtain a curve. This curve stands for NFmin of the combination of V_{bias} and W that meet the power requirement. From it, the optimal combination of W and V_{bias} can be obtained. In Fig. 8, sub-step 3 shows this step. The optimal combination is 220 μm W and 0.575 V V_{bias}. Its NFmin is only 0.78 dB, 0.265 dB smaller than that obtained though PCSNIM.

Step 3: Set L_g's parasitic resistance (R_{Lg}) and L_s. $\mathrm{Im}[Z_{opt}]$ of the circuit can be seen as an approximate value of L_g. According to the bond inductor's quality factor (about 75 at 2.4 GHz), a rough vaule of R_{Lg} can be obtained, and it will be adjusted in Step 6. Set the initial value of L_s to a value not too large (e.g. 1 nH) and it will be tuned in Step 4. Large L_s will reduce the power gain and worsen the noise performance.

Step 4: Set the value of L_g to 0. Tune C_{ex} and L_s to satisfy the equation $\mathrm{Re}[Z_{opt}] = \mathrm{Re}[Z_{in}] = 50\ \Omega$. Due to the effect of C_p, usually $\mathrm{Re}[Z_{in}]$ is much less than 50 Ω, while $\mathrm{Re}[Z_{opt}]$ is still more than it. According to Eq. (5) and the description above, it will make $\mathrm{Re}[Z_{in}]$ increase and $\mathrm{Re}[Z_{opt}]$ decrease to increase C_{ex}. So $\mathrm{Re}[Z_{opt}] = \mathrm{Re}[Z_{in}] = 50\ \Omega$ will be achieved by choosing a proper value for C_{ex}. If even a very large value of C_{ex} can't make $\mathrm{Re}[Z_{in}]$ match 50 Ω, increase the value of L_s appropriately and rechoose the value of C_{ex}. The process is shown in Fig. 9.

Step 5: Calculate the value of L_g according to simulated $\mathrm{Im}[Z_{opt}]$ in Fig. 9. After setting L_g to that value, $\mathrm{Im}[Z_{opt}]$ will move down along the 50 Ω circle, while $\mathrm{Im}[Z_{in}]$ will change in the opposite direction. They will meet at the origin because the imaginary parts of Z_{opt} and Z_{in} are almost equal. The change process of S11 and Z_{opt} is shown in Fig. 10.

Step 6: Calculate L_g's parasitic resistance according to its quality factor and set it to that value.

Step 7: Repeat Step 4, until the input power matching and noise matching can be achieved simultaneously through a fine tuning of L_g.

Step 8: If Step 7 can't be achieved, make a tuning of V_{bias} and W, and then repeat Steps 4 to 7. As Figure 8 shows, the increase in NFmin is very slight because of a small tuning of V_{bias}.

The values of C_{ex}, L_g and L_s, obtained after these steps, are 64 fF, 6.8 nH and 1 nH, respectively. The simulated results are shown in Figs. 11 and 12. As can be seen in these figures, in addition to good input matching, the NF of the designed LNA coincides with the NFmin at a frequency of 2.4 GHz. So the

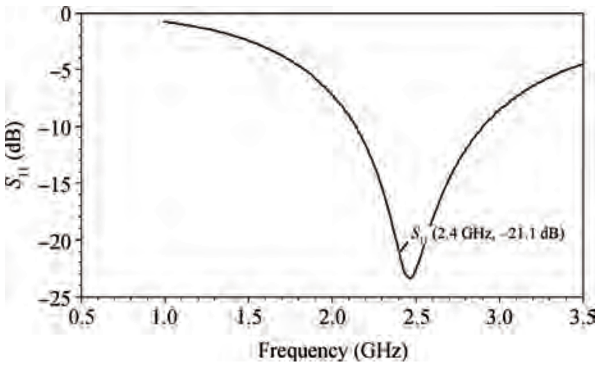

Fig. 12. Simulated S_{11}.

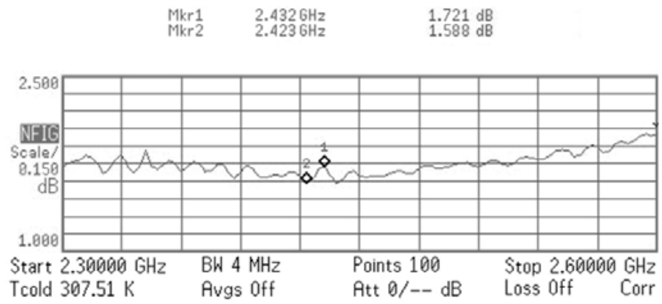

Fig. 15. Measured noise figure.

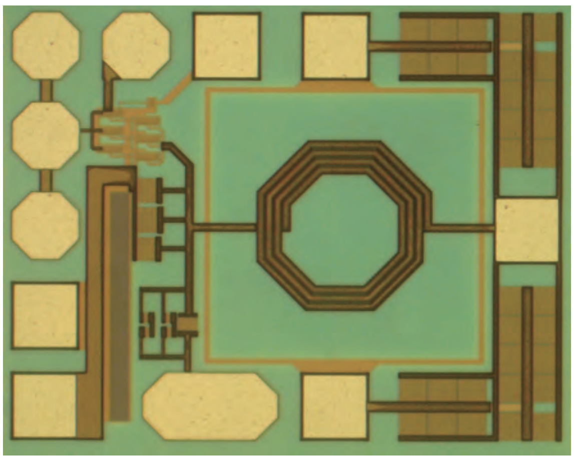

Fig. 13. Micrograph of the LNA with ESD.

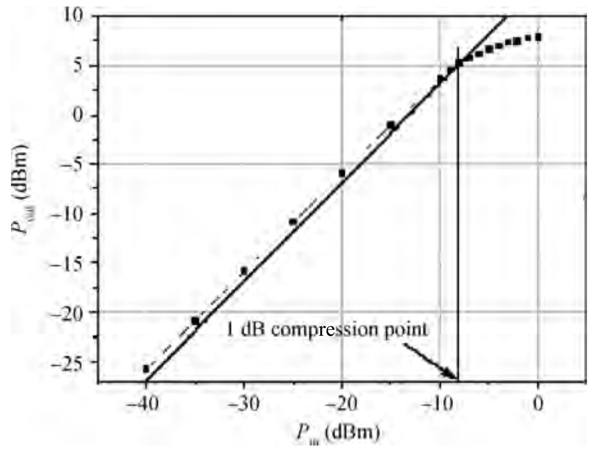

Fig. 16. Measured input 1-dB compression point.

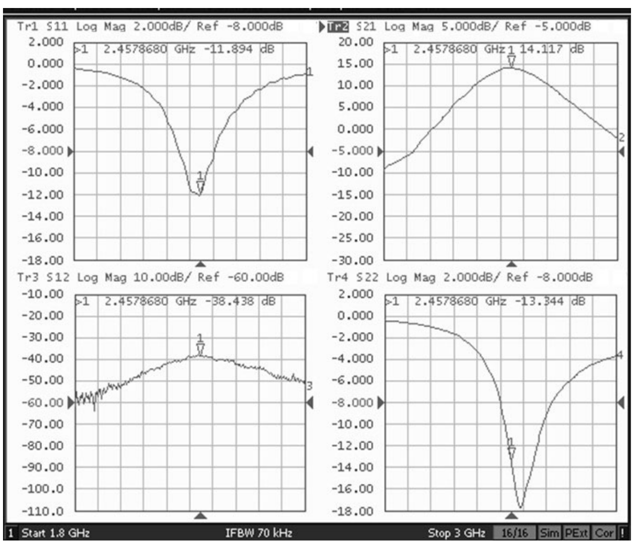

Fig. 14. Measured S-parameter.

ESD protected LNA's power-constrained simultaneous noise and input matching are realized.

3.3. Measured results

The micrograph of the LNA with ESD is shown in Fig. 13. The chip area including all bonding pads is 470×600 μm^2.

The chip was measured in the test laboratory of the Institute of RF- & OE-ICs, Southeast University. The major test equipment includes an Agilent network analyzer E5071B, a spectrum analyzer E4440A, an RF signal generator E4438C and a noise figure analyzer N8975A. The measured DC current is about 4 mA under a supply of 1.8 V.

Figure 14 shows the measured results of the S-parameter. It can be observed that both the input and output impedance matching value, S_{11} and S_{22}, are below -11 dB. The maximum power gain of the LNA is 14.12 dB at a frequency of 2.45 GHz.

Figure 15 shows the measured result of the noise figure. The minimum value of NF is 1.59 dB at 2.42 GHz, while the maximum value is 1.72 dB at 2.43 GHz. In most of the frequency range, the noise figure is below 1.7 dB.

The input 1 dB compression point is –8 dBm, as can be seen in Fig. 16. It is obtained with the dot method after recording the input powers and corresponding output powers.

IIP3 is obtained with the double tone multi-frequency (DTMF) test method with –23 dBm input power. The result is shown in Fig. 17 and the IIP3 is about 1 dBm.

Table 1 gives the measured results of the LNA in detail and a comparison with recently published LNAs operated at the same frequency of 2.4 GHz. From this table we can conclude that the key figures of the LNA designed in this paper are superior to those of others.

Table 1. Performance comparisons with recently published LNAs.

Ref.	Power gain (dB)	NF (dB)	S_{11} (dB)	P_{dc} (mW)	IIP3 (dBm)	Process (nm)
[6]	21.9	2.56	–12.6	12.9	–11	90 CMOS
[7]	13.0	3.60	–13.0	6.5	NA	130 SOI CMOS
[8]	12.1	2.77	–20.0	4.5	2.4	150 CMOS
[9]	10.5	4.80	–14.0	17.5	NA	250 CMOS
This work	14.12	1.59	–11	7.2	1	180 CMOS

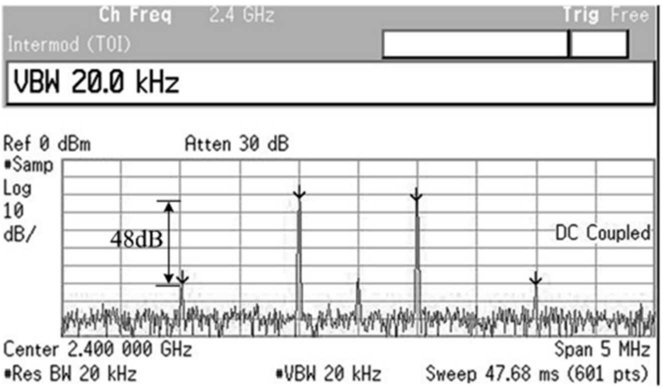

Fig. 17. Result of DTMF detection test.

4. Conclusions

In this paper, the method of PCSNIM with ESD is proposed. In addition, the input impedance and noise parameters of the LNA with ESD protection circuit are analyzed in detail. Based on this method, an LNA for 2.4 GHz WSN applications is presented. The measured results show that the proposed optimization technology is available.

Appendix A

The derivation of the source inductance degenerated CS LNA's optimum source admittance ($Y_{\rm opt}$) is as follows.

In Fig. A1, $\overline{i_{\rm nd}^2}$ is the channel thermal noise, $\overline{i_{\rm ng}^2}$ is the drain induced gate noise, and $\overline{v_{\rm n}^2}$ and $\overline{i_{\rm n}^2}$ are the equivalent input noise voltage and current, respectively.

From Fig. A1, $\overline{v_{\rm n}^2}$ and $\overline{i_{\rm n}^2}$ can be worked out,

$$\begin{cases} i_{\rm n} = -\dfrac{sC_{\rm gs}}{g_{\rm m}}\left(\alpha\,|c|\sqrt{\dfrac{\delta}{5\gamma}}+1\right)i_{\rm nd}-i_{\rm ngu}, \\ v_{\rm n} = -\dfrac{1}{g_{\rm m}}\left[s^2C_{\rm gs}(L_{\rm g}+L_{\rm s})\left(\alpha\,|c|\sqrt{\dfrac{\delta}{5\gamma}}+1\right)+1\right]i_{\rm nd} \\ \qquad -s(L_{\rm g}+L_{\rm s})i_{\rm ngu}, \end{cases}$$

where

$$\alpha \triangleq \frac{g_{\rm m}}{g_{\rm d0}},$$

where $g_{\rm m}$ is the device transconductance, and $g_{\rm d0}$ is the zero-bias drain conductance. γ is the coefficient of channel thermal noise. δ is the coefficient of gate noise, and

$$c = \frac{\overline{i_{\rm g}i_{\rm d}^*}}{\sqrt{\overline{i_{\rm g}^2}\,\overline{i_{\rm d}^2}}} \approx 0.395{\rm j},$$

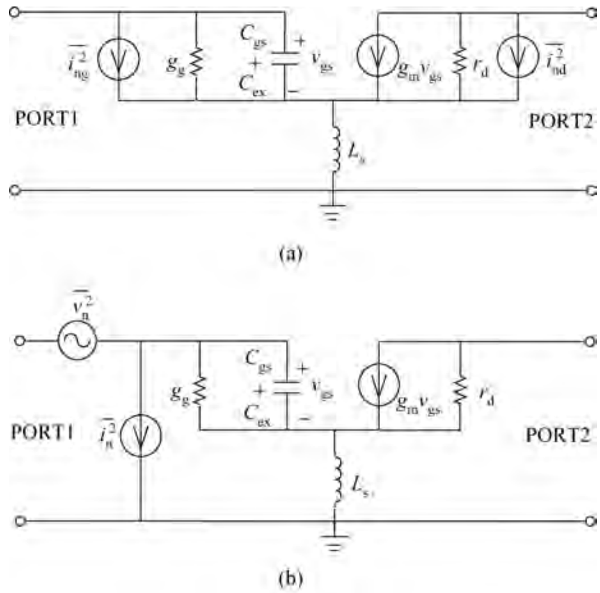

Fig. A1. (a) Noise model of the source inductance degenerated CS LNA. (b) Equivalent input noise voltage and current model with noiseless network.

$$i_{\rm ngu} = i_{\rm ng} - i_{\rm ngc},$$

where $i_{\rm ngu}$, $i_{\rm ngc}$ are the unrelated and related parts between $i_{\rm nd}$ and $i_{\rm ng}$.

Let

$$\begin{aligned} R_{\rm n} &= \frac{\overline{v_{\rm n}^2}}{4kT\Delta f} \\ &= \frac{\gamma}{\alpha g_{\rm m}}\Big[1+\omega^4C_{\rm gs}^2(L_{\rm g}+L_{\rm s})^2 \\ &\quad \times\left(2\alpha\,|c|\sqrt{\frac{\delta}{5\gamma}}+\frac{\alpha^2\delta}{5\gamma}+1\right)\Big] \\ &\quad -\frac{\gamma}{\alpha g_{\rm m}}\left[2\omega^2C_{\rm gs}(L_{\rm g}+L_{\rm s})\left(\alpha\,|c|\sqrt{\frac{\delta}{5\gamma}}+1\right)\right]. \end{aligned}$$

$Y_{\rm c}$ stands for the correlation coefficient between $v_{\rm n}$ and $i_{\rm n}$, and is defined as

$$Y_{\rm c} = c'^*\sqrt{\frac{\overline{i_{\rm n}^2}}{\overline{v_{\rm n}^2}}} = \frac{\overline{v_{\rm n}i_n^*}}{\sqrt{\overline{v_{\rm n}^2i_{\rm n}^2}}}\sqrt{\frac{\overline{i_{\rm n}^2}}{\overline{v_{\rm n}^2}}} = \frac{\overline{v_{\rm n}i_{\rm n}^*}}{\overline{v_{\rm n}^2}},$$

$$Y_{\mathrm{c}}=\frac{sC_{\mathrm{gs}}\left(\alpha\left|c\right|\sqrt{\frac{\delta}{5\gamma}}+1\right)-\omega^{2}C_{\mathrm{gs}}^{2}sL_{\mathrm{s}}\left(2\alpha\left|c\right|\sqrt{\frac{\delta}{5\gamma}}+1+\frac{\alpha^{2}\delta}{5\gamma}\right)}{1+\omega^{4}C_{\mathrm{gs}}^{2}L_{\mathrm{s}}^{2}\left(2\alpha\left|c\right|\sqrt{\frac{\delta}{5\gamma}}+1+\frac{\alpha^{2}\delta}{5\gamma}\right)-2\omega^{2}C_{\mathrm{gs}}L_{\mathrm{s}}\left(\alpha\left|c\right|\sqrt{\frac{\delta}{5\gamma}}+1\right)}$$

$$=\frac{\mathrm{j}\omega C_{\mathrm{gs}}\left(\alpha\left|c\right|\sqrt{\frac{\delta}{5\gamma}}+1\right)-\mathrm{j}\omega^{3}C_{\mathrm{gs}}^{2}L_{\mathrm{s}}\left(2\alpha\left|c\right|\sqrt{\frac{\delta}{5\gamma}}+1+\frac{\alpha^{2}\delta}{5\gamma}\right)}{1+\omega^{4}C_{\mathrm{gs}}^{2}L_{\mathrm{s}}^{2}\left(2\alpha\left|c\right|\sqrt{\frac{\delta}{5\gamma}}+1+\frac{\alpha^{2}\delta}{5\gamma}\right)-2\omega^{2}C_{\mathrm{gs}}L_{\mathrm{s}}\left(\alpha\left|c\right|\sqrt{\frac{\delta}{5\gamma}}+1\right)}$$

$$=\mathrm{j}\frac{\omega C_{\mathrm{gs}}\left(\alpha\left|c\right|\sqrt{\frac{\delta}{5\gamma}}+1\right)-\omega^{3}C_{\mathrm{gs}}^{2}L_{\mathrm{s}}\left(2\alpha\left|c\right|\sqrt{\frac{\delta}{5\gamma}}+1+\frac{\alpha^{2}\delta}{5\gamma}\right)}{1+\omega^{4}C_{\mathrm{gs}}^{2}L_{\mathrm{s}}^{2}\left(2\alpha\left|c\right|\sqrt{\frac{\delta}{5\gamma}}+1+\frac{\alpha^{2}\delta}{5\gamma}\right)-2\omega^{2}C_{\mathrm{gs}}L_{\mathrm{s}}\left(\alpha\left|c\right|\sqrt{\frac{\delta}{5\gamma}}+1\right)}$$

$$=G_{\mathrm{c}}+\mathrm{j}B_{\mathrm{c}}=\mathrm{j}B_{\mathrm{c}},$$

so

$$B_{\mathrm{c}}=\frac{\omega C_{\mathrm{gs}}\left(\alpha\left|c\right|\sqrt{\frac{\delta}{5\gamma}}+1\right)-\omega^{3}C_{\mathrm{gs}}^{2}L_{\mathrm{s}}\left(2\alpha\left|c\right|\sqrt{\frac{\delta}{5\gamma}}+1+\frac{\alpha^{2}\delta}{5\gamma}\right)}{1+\omega^{4}C_{\mathrm{gs}}^{2}L_{\mathrm{s}}^{2}\left(2\alpha\left|c\right|\sqrt{\frac{\delta}{5\gamma}}+1+\frac{\alpha^{2}\delta}{5\gamma}\right)-2\omega^{2}C_{\mathrm{gs}}L_{\mathrm{s}}\left(\alpha\left|c\right|\sqrt{\frac{\delta}{5\gamma}}+1\right)},$$

$$G_{\mathrm{c}}=0.$$

According to Y_{c}, the unrelated part between v_{n} and i_{n} can be calculated. It is

$$i_{\mathrm{nu}}=i_{\mathrm{n}}-i_{\mathrm{nc}}=i_{\mathrm{n}}-Y_{\mathrm{c}}v_{\mathrm{n}}$$

$$=-\frac{sC_{\mathrm{gs}}}{g_{\mathrm{m}}}\left(\alpha\left|c\right|\sqrt{\frac{\delta}{5\gamma}}+1\right)i_{\mathrm{nd}}-i_{\mathrm{ngu}}+Y_{\mathrm{c}}\left\{\frac{1}{g_{\mathrm{m}}}\left[s^{2}C_{\mathrm{gs}}L_{\mathrm{s}}\left(\alpha\left|c\right|\sqrt{\frac{\delta}{5\gamma}}+1\right)+1\right]i_{\mathrm{nd}}+sL_{\mathrm{s}}i_{\mathrm{ngu}}\right\}$$

$$=\left\{\frac{Y_{\mathrm{c}}}{g_{\mathrm{m}}}\left[s^{2}C_{\mathrm{gs}}L_{\mathrm{s}}\left(\alpha\left|c\right|\sqrt{\frac{\delta}{5\gamma}}+1\right)+1\right]-\frac{sC_{\mathrm{gs}}}{g_{\mathrm{m}}}\left(\alpha\left|c\right|\sqrt{\frac{\delta}{5\gamma}}+1\right)\right\}i_{\mathrm{nd}}+\left(Y_{\mathrm{c}}sL_{\mathrm{s}}-1\right)i_{\mathrm{ngu}}.$$

$$G_{\mathrm{u}}=\frac{\overline{i_{\mathrm{nu}}^{2}}}{4kT\Delta f}$$

$$=\left|\frac{Y_{\mathrm{c}}}{g_{\mathrm{m}}}\left[s^{2}C_{\mathrm{gs}}L_{\mathrm{s}}\left(\alpha\left|c\right|\sqrt{\frac{\delta}{5\gamma}}+1\right)+1\right]-\frac{sC_{\mathrm{gs}}}{g_{\mathrm{m}}}\left(\alpha\left|c\right|\sqrt{\frac{\delta}{5\gamma}}+1\right)\right|^{2}\frac{\overline{i_{\mathrm{nd}}^{2}}}{4kT\Delta f}+\left|Y_{\mathrm{c}}sL_{\mathrm{s}}-1\right|^{2}\frac{\overline{i_{\mathrm{ngu}}^{2}}}{4kT\Delta f}$$

$$=\left|\frac{Y_{\mathrm{c}}}{g_{\mathrm{m}}}\left[1-\omega^{2}C_{\mathrm{gs}}L_{\mathrm{s}}\left(\alpha\left|c\right|\sqrt{\frac{\delta}{5\gamma}}+1\right)\right]-\frac{\mathrm{j}\omega C_{\mathrm{gs}}}{g_{\mathrm{m}}}\left(\alpha\left|c\right|\sqrt{\frac{\delta}{5\gamma}}+1\right)\right|^{2}\gamma g_{\mathrm{d0}}+\left|\mathrm{j}\omega Y_{\mathrm{c}}L_{\mathrm{s}}-1\right|^{2}\delta g_{\mathrm{g}}\left(1-\left|c\right|^{2}\right)$$

$$=\left|\frac{\mathrm{j}B_{\mathrm{c}}}{g_{\mathrm{m}}}\left[1-\omega^{2}C_{\mathrm{gs}}L_{\mathrm{s}}\left(\alpha\left|c\right|\sqrt{\frac{\delta}{5\gamma}}+1\right)\right]-\frac{\mathrm{j}\omega C_{\mathrm{gs}}}{g_{\mathrm{m}}}\left(\alpha\left|c\right|\sqrt{\frac{\delta}{5\gamma}}+1\right)\right|^{2}\gamma g_{\mathrm{d0}}+\left|\omega B_{\mathrm{c}}L_{\mathrm{s}}+1\right|^{2}\delta g_{\mathrm{g}}\left(1-\left|c\right|^{2}\right)$$

$$= \left| \frac{B_\mathrm{c}}{g_\mathrm{m}} \left[1 - \omega^2 C_\mathrm{gs} L_\mathrm{s} \left(\alpha |c| \sqrt{\frac{\delta}{5\gamma}} + 1 \right) \right] - \frac{\omega C_\mathrm{gs}}{g_\mathrm{m}} \left(\alpha |c| \sqrt{\frac{\delta}{5\gamma}} + 1 \right) \right|^2 \gamma g_\mathrm{d0} + |\omega B_\mathrm{c} L_\mathrm{s} + 1|^2 \delta g_\mathrm{g} \left(1 - |c|^2 \right)$$

$$= \frac{\gamma g_\mathrm{d0} B_\mathrm{c}^2}{g_\mathrm{m}^2} \left[1 - \omega^2 C_\mathrm{gs} L_\mathrm{s} \left(\alpha |c| \sqrt{\frac{\delta}{5\gamma}} + 1 \right) \right]^2 + \frac{\gamma g_\mathrm{d0} \omega^2 C_\mathrm{gs}^2}{g_\mathrm{m}^2} \left(\alpha |c| \sqrt{\frac{\delta}{5\gamma}} + 1 \right)^2$$
$$- 2 \frac{\gamma g_\mathrm{d0} \omega C_\mathrm{gs}}{g_\mathrm{m}} \left(\alpha |c| \sqrt{\frac{\delta}{5\gamma}} + 1 \right) \frac{B_\mathrm{c}}{g_\mathrm{m}} \left[1 - \omega^2 C_\mathrm{gs} L_\mathrm{s} \left(\alpha |c| \sqrt{\frac{\delta}{5\gamma}} + 1 \right) \right]$$
$$+ \left(\omega^2 B_\mathrm{c}^2 L_\mathrm{s}^2 + 1 + 2\omega B_\mathrm{c} L_\mathrm{s} \right) \delta \frac{\omega^2 C_\mathrm{gs}^2}{5 g_\mathrm{d0}} \left(1 - |c|^2 \right).$$

$$G_\mathrm{u} = \frac{\gamma g_\mathrm{d0} B_\mathrm{c}^2}{g_\mathrm{m}^2} - 2 \frac{\gamma g_\mathrm{d0} B_\mathrm{c}^2}{g_\mathrm{m}^2} \omega^2 C_\mathrm{gs} L_\mathrm{s} \left(\alpha |c| \sqrt{\frac{\delta}{5\gamma}} + 1 \right) + \frac{\gamma g_\mathrm{d0} B_\mathrm{c}^2}{g_\mathrm{m}^2} \omega^4 C_\mathrm{gs}^2 L_\mathrm{s}^2 \left(\alpha^2 |c|^2 \frac{\delta}{5\gamma} + 2\alpha |c| \sqrt{\frac{\delta}{5\gamma}} + 1 \right)$$
$$+ \frac{\gamma g_\mathrm{d0} \omega^2 C_\mathrm{gs}^2}{g_\mathrm{m}^2} \left(\alpha^2 |c|^2 \frac{\delta}{5\gamma} + 2\alpha |c| \sqrt{\frac{\delta}{5\gamma}} + 1 \right)$$
$$- 2 \frac{\gamma g_\mathrm{d0} \omega C_\mathrm{gs}}{g_\mathrm{m}^2} B_\mathrm{c} \left(\alpha |c| \sqrt{\frac{\delta}{5\gamma}} + 1 \right) \left[1 - \omega^2 C_\mathrm{gs} L_\mathrm{s} \left(\alpha |c| \sqrt{\frac{\delta}{5\gamma}} + 1 \right) \right]$$
$$+ \left[\omega^2 B_\mathrm{c}^2 L_\mathrm{s}^2 + 1 + 2\omega B_\mathrm{c} L_\mathrm{s} \right] \delta \frac{\omega^2 C_\mathrm{gs}^2}{5 g_\mathrm{d0}} \left(1 - |c|^2 \right)$$
$$= \frac{\gamma B_\mathrm{c}^2}{\alpha g_\mathrm{m}} - \frac{1}{g_\mathrm{m}} \frac{2\gamma}{\alpha} B_\mathrm{c}^2 \omega^2 C_\mathrm{gs} L_\mathrm{s} \left(\alpha |c| \sqrt{\frac{\delta}{5\gamma}} + 1 \right)$$
$$+ B_\mathrm{c}^2 \omega^4 C_\mathrm{gs}^2 L_\mathrm{s}^2 \left(\alpha^2 |c|^2 \frac{\delta}{5\gamma} \frac{\gamma}{\alpha g_\mathrm{m}} + 2\alpha |c| \sqrt{\frac{\delta}{5\gamma}} \frac{\gamma}{\alpha g_\mathrm{m}} + \frac{\gamma}{\alpha g_\mathrm{m}} \right)$$
$$+ \frac{\gamma \omega^2 C_\mathrm{gs}^2}{\alpha g_\mathrm{m}} \left(\alpha^2 |c|^2 \frac{\delta}{5\gamma} + 2\alpha |c| \sqrt{\frac{\delta}{5\gamma}} + 1 \right) - 2 \frac{\gamma \omega C_\mathrm{gs}}{\alpha g_\mathrm{m}} B_\mathrm{c} \left(\alpha |c| \sqrt{\frac{\delta}{5\gamma}} + 1 \right)$$
$$+ 2 \frac{\gamma}{\alpha g_\mathrm{m}} B_\mathrm{c} \omega^3 C_\mathrm{gs}^2 L_\mathrm{s} \left(\alpha^2 |c|^2 \frac{\delta}{5\gamma} + 2\alpha |c| \sqrt{\frac{\delta}{5\gamma}} + 1 \right)$$
$$+ B_\mathrm{c}^2 \omega^4 C_\mathrm{gs}^2 L_\mathrm{s}^2 \left(\frac{\delta}{5 g_\mathrm{d0}} - |c|^2 \frac{\delta}{5 g_\mathrm{d0}} \right) + \frac{\gamma}{\alpha g_\mathrm{m}} \omega^2 C_\mathrm{gs}^2 \left(\frac{\alpha^2 \delta}{5\gamma} - |c|^2 \frac{\alpha^2 \delta}{5\gamma} \right) + B_\mathrm{c} \omega^3 C_\mathrm{gs}^2 L_\mathrm{s} \left(2 \frac{\delta}{5 g_\mathrm{d0}} - |c|^2 2 \frac{\delta}{5 g_\mathrm{d0}} \right)$$
$$= \frac{1}{g_\mathrm{m}} B_\mathrm{c}^2 \omega^4 C_\mathrm{gs}^2 L_\mathrm{s}^2 \left(2 |c| \sqrt{\frac{\delta\gamma}{5}} + \frac{\alpha\delta}{5} + \frac{\gamma}{\alpha} \right) + \frac{1}{g_\mathrm{m}} B_\mathrm{c} \omega^3 C_\mathrm{gs}^2 L_\mathrm{s} \left(4 |c| \sqrt{\frac{\delta\gamma}{5}} + \frac{2\gamma}{\alpha} + \frac{2\alpha\delta}{5} \right)$$
$$- \frac{1}{g_\mathrm{m}} \frac{2\gamma}{\alpha} B_\mathrm{c}^2 \omega^2 C_\mathrm{gs} L_\mathrm{s} \left(\alpha |c| \sqrt{\frac{\delta}{5\gamma}} + 1 \right) + \frac{\gamma}{\alpha g_\mathrm{m}} \omega^2 C_\mathrm{gs}^2 \left(2\alpha |c| \sqrt{\frac{\delta}{5\gamma}} + 1 + \frac{\alpha^2 \delta}{5\gamma} \right)$$
$$- 2 \frac{\gamma}{\alpha g_\mathrm{m}} B_\mathrm{c} \omega C_\mathrm{gs} \left(\alpha |c| \sqrt{\frac{\delta}{5\gamma}} + 1 \right) + \frac{\gamma B_\mathrm{c}^2}{\alpha g_\mathrm{m}}.$$

So, Y_opt can be worked out.

$$
\begin{aligned}
G_{\rm opt} &= \sqrt{G_{\rm c}^2+\frac{G_{\rm u}}{R_{\rm n}}} = \sqrt{0+\frac{G_{\rm u}}{R_{\rm n}}} = \sqrt{\frac{G_{\rm u}}{R_{\rm n}}} \\
&= \left[B_{\rm c}^2\omega^4C_{\rm t}^2L_{\rm s}^2\left(2\alpha\left|c\right|\sqrt{\frac{\delta}{5\gamma}}+\frac{\alpha^2\delta}{5\gamma}+1\right)+2B_{\rm c}\omega^3C_{\rm t}^2L_{\rm s}\left(2\alpha\left|c\right|\sqrt{\frac{\delta}{5\gamma}}+1+\frac{\alpha^2\delta}{5\gamma}\right)\right. \\
&\quad -2B_{\rm c}^2\omega^2C_{\rm t}L_{\rm s}\left(\alpha\left|c\right|\sqrt{\frac{\delta}{5\gamma}}+1\right)+\omega^2C_{\rm t}^2\left(2\alpha\left|c\right|\sqrt{\frac{\delta}{5\gamma}}+1+\frac{\alpha^2\delta}{5\gamma}\right) \\
&\quad \left.-2B_{\rm c}\omega C_{\rm t}\left(\alpha\left|c\right|\sqrt{\frac{\delta}{5\gamma}}+1\right)+B_{\rm c}^2\right]^{1/2} \\
&\quad \times\left[1+\omega^4C_{\rm t}^2L_{\rm s}^2\left(2\alpha\left|c\right|\sqrt{\frac{\delta}{5\gamma}}+\frac{\alpha^2\delta}{5\gamma}+1\right)-2\omega^2C_{\rm t}L_{\rm s}\left(\alpha\left|c\right|\sqrt{\frac{\delta}{5\gamma}}+1\right)\right]^{-1/2}.
\end{aligned}
$$

$$
\begin{aligned}
B_{\rm opt} &= -B_{\rm c} \\
&= -\frac{\omega C_{\rm t}\left(\alpha\left|c\right|\sqrt{\frac{\delta}{5\gamma}}+1\right)-\omega^3C_{\rm t}^2L_{\rm s}\left(2\alpha\left|c\right|\sqrt{\frac{\delta}{5\gamma}}+1+\frac{\alpha^2\delta}{5\gamma}\right)}{1+\omega^4C_{\rm t}^2L_{\rm s}^2\left(2\alpha\left|c\right|\sqrt{\frac{\delta}{5\gamma}}+1+\frac{\alpha^2\delta}{5\gamma}\right)-2\omega^2C_{\rm t}L_{\rm s}\left(\alpha\left|c\right|\sqrt{\frac{\delta}{5\gamma}}+1\right)}.
\end{aligned}
$$

$$
Y_{\rm opt} = G_{\rm opt}+{\rm j}B_{\rm opt}.
$$

References

[1] Shaeffer D K, Lee T H. A 1.5 V, 1.5 GHz CMOS low noise amplifier. IEEE J Solid-State Circuits, 1997, 32(5): 745

[2] Nguyen T K, Kin C H, Ihm G J, et al. CMOS low-noise amplifier design optimization techniques. IEEE Trans Microw Theory Tech, 2004, 52 (5): 1433

[3] Chandrasekhar V, Mayaram K. Analysis of CMOS RF LNAs with ESD protection. IEEE International Symposium on Circuits and System, 2002: 779

[4] Sivonen P, Parssinen A. Analysis and optimization of packaged inductively degenerated common-source low noise amplifiers with ESD protection. IEEE Trans Microw Theory Tech, 2005, 53(4): 1304

[5] Richier C, Salome P, Mabboux G, et al. Investigation on different ESD protection strategies devoted to 3.3 V RF applications (2 GHz) in a 0.18 μm CMOS process. EOS/ESD Symposium Proceeding, California, USA, 2000: 251

[6] Chang C P, Hou J A, Su J, et al. A high gain and low supply voltage LNA for the direct conversion application with 4-kV HBM ESD protection in 90-nm RF CMOS. IEEE Microw Wireless Compon Lett, 2006, 16(11): 188

[7] Kaamouchi M E, Moussa M S, Delatte P, et al. A 2.4-GHz fully integrated ESD-protection low noise amplifier in 130-nm PD SOI CMOS technology. IEEE Trans Microw Theory Tech, 2007, 55(12): 2822

[8] Chandrasekhar V, Hung C M, Ho Y C, et al. A packaged 2.4 GHz LNA in a 0.15 μm CMOS process with 2 kV HBM ESD protection. Proceedings of the 28th European Solid-State Circuits Conference, Florence, Italy, 2002: 347

[9] Bo-Shih H, Ming-Dou K. New matching methodology of low-noise amplifier with ESD protection. IEEE International Symposium on Circuits and Systems, Island of Kos, Greece, 2006: 4891